The Boreal Aurora Camera Constellation (BACC) – Status 2025

F. Sigernes [1, *], M. Syrjäsuo [1], E. Trondsen [2], J. B. Carlsen [2], L. Clausen [2,*], M. Kellinsalmi [3],
K. Kauristie [3, *], M. G. Johnsen [4, *], M. Flügge [5,*] and A. Danielsen [5]

[1] The University Centre in Svalbard (UNIS), N-9171 Longyearbyen, Norway

[2] Department of physics, University of Oslo, Norway

[3] Finnish Meteorological Institute, Helsinki, Finland

[4] Tromsø Geophysical Observatory (TGO), The Arctic University of Norway[4]

[5] Alomar Observatory, Andøya Space (AS), Norway.

[*] Prime Investigators

Abstract

This project describes the deployment of a low-cost all-sky color camera network to study auroral morphology and weather from multiple locations. The main goal is to obtain a tool to nowcast and map in real time dark sky conditions, including phenomena like auroras, meteor strikes and solar or moon illuminated high altitude clouds. Two camera stations at Svalbard have been operational at the Kjell Henriksen Observatory ([KHO](#)) and in Ny-Ålesund since 2015. Two more were deployed to Kevo and Muonio in northern Finland in 2017. In 2020, one more was installed at the old Skibotn Observatory. The last camera was installed in November 2025 at the Alomar Observatory at Andøya Space. The plan is to further utilize existing auroral boreal infrastructure to create a constellation of cameras.

1. Introduction

The arrival of new image sensors with increased light sensitivity like the back illuminated CMOS (Complementary Metal-Oxide Semiconductors) chip, makes it possible to construct a new generation of low-cost camera systems that can detect aurora and other dark sky phenomena in full color. In fact, the availability of these new detectors enables us to operate instruments under any background sky conditions including scattered light pollution and cloud cover. A fully operative multi-site network of cameras will sample a large portion of the auroral oval. It will therefore be used to validate and improve our [forecasting service](#).[1]

Automated classification of the sky conditions including cloudiness, clear sky or visible aurora is a non-trivial challenge.[2-6] The main difficulties include the ambiguity of the apparent shapes of the auroral display observed from different locations and the changing background sky spectrum. The use of color opens new opportunities. It is now possible to detect and classify night sky objects based on f. ex. color matching algorithms using numeric features extracted

from real-time images. Therefore, we propose to introduce a camera network where data from each camera station will be analyzed in real time. Note that human visual inspection of the data is valuable for focused actions such as radar and rocket campaigns.

A low-cost all-sky color CMOS camera has been assembled and tested at KHO. Data from this instrument will be presented to illustrate the above points.

2. The camera station

The core of the instrument is the back illuminated Sony Exmor IMX174 CMOS sensor. The company ZWO has produced a compact camera head (model ASI174MC) based on the IMX174 sensor that is aimed for the astrophysical marked. It features a global electronic shutter with no moving mechanical parts. The diagonal of the sensor is 13.4 mm with 1936 x 1216 pixels of size 5.86 µm. Peak quantum efficiency is 78% at 500 nm. The camera is powered by the USB port.

Figure 1 show a technical drawing of the camera head. The C-mount Fujinon F/1.4 fish-eye lens (FE185C057HA-1) is used as front optic. The lens has a field of view of 185° and an image diameter of 5.7 mm, which is well within the area of the sensor. A T2 to C-mount ring adapter is used to mount the lens to the camera head.
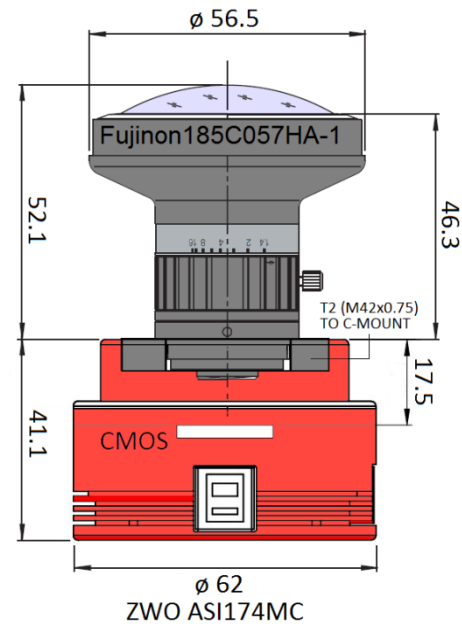

Fig. 1 Drawing of the ZWO ASI174MC camera head and the Fujinon F/1.4 all-sky lens. All measurements are in mm.

The camera is controlled by a computer that is operated by Windows. ZWO provides a SDK to operate the camera by the language C+. A Pascal translation has been conducted to be able to use Delphi from Embarcadero. The software, named ZWOASI174MC.exe, is a standalone 64-bit program that is tested to run stable with no memory leaks. It produces compass overlaid frames and Xvid compressed AVI movies with structured naming rules based on time and date. Frame accumulation is included to reduce noise. Daily Keograms, Stack plots and Quick looks are generated to view the sky activity over time.

The camera is protected from direct sun light by a 3D printed lid / shutter, controlled by an Arduino microcomputer and a standard Parallax servo.

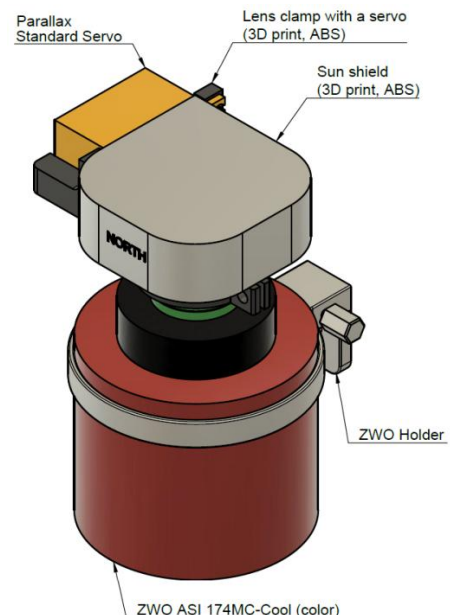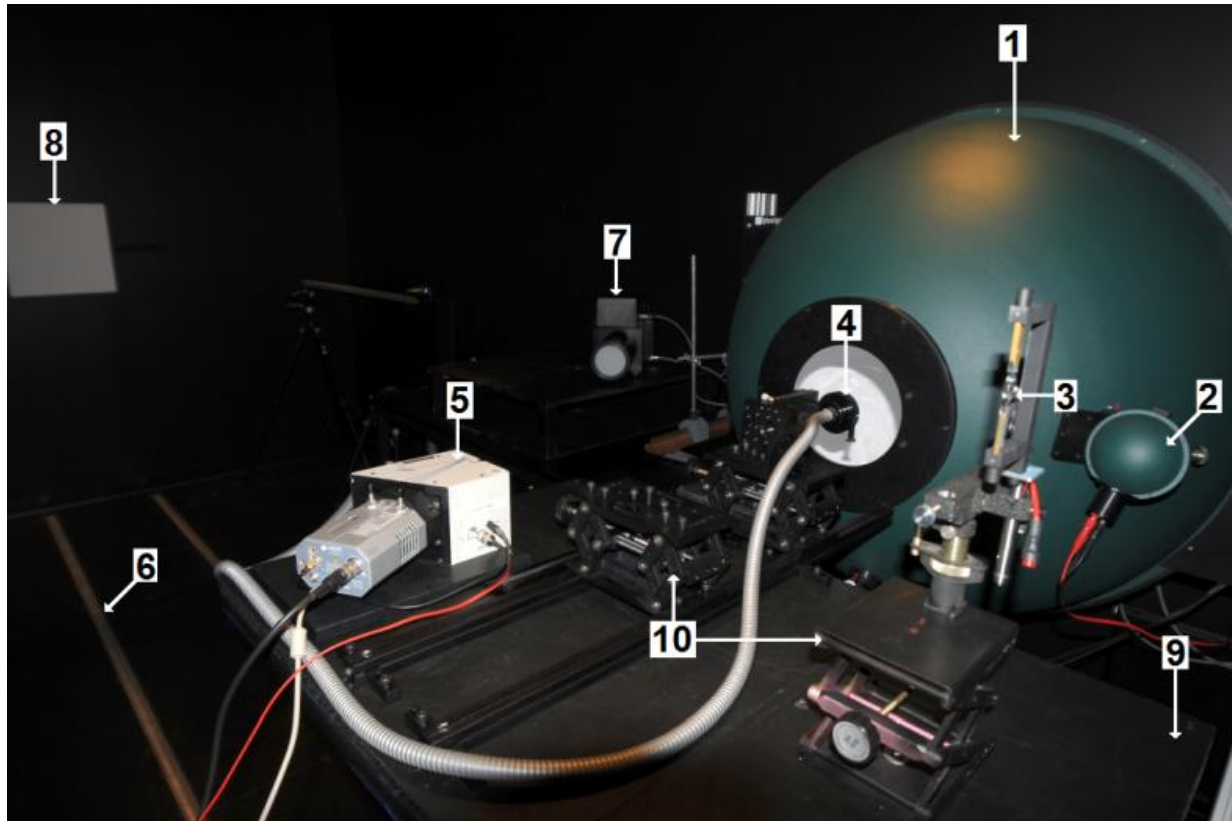**Fig. 2** Drawing of the ZWO ASI174MC Cooled

UNIVERSITY CENTRE IN SVALBARD UNIS BOX 156 9171 LONGYEARBYEN NORWAY

camera head with Sun protection.

Fig. 3. Experimental setup at UNIS optical lab: (1) Labsphere 1 m diameter integrating sphere, (2) source lamp sphere, (3) Oriel 45 W tungsten Lamp (FEL), (4) fiber bundle probe, (5) Oriel FICS 77443 spectrograph, (6) rail road, (7) Keo Alcor-RC lamp, (8) Lambertian screen, (9) adjustable table on rails, and (10) table jacks.

Figure 2 shows the technical drawing of the shutter protection system. The servo and the microcomputer are both powered by a second USB port. Serial communication (RS-232) is used to open or close the shutter according to the maximum solar elevation angle allowed at the site. A typical solar elevation angle of 10 degrees below the horizon is a safe limit to avoid overexposure and damage to the sensors.

3. Sensitivity and laboratory work

The camera will be calibrated at the UNIS calibration laboratory. Figure 3 shows some the calibration tools[6] available for the project at the laboratory. A three-step method to calibrate and characterize each color channel of the camera is outlined below:

1. Focus and the radial mapping function of the all-sky lens will be measured by a rotating arm with a 10 μm pinhole source at distance 1 m. Night sky star constellations will be used to verify the calibration.
2. Flat-field correction or off-axis response of the camera will be conducted using a modified l m diameter integrating sphere.[8]
3. The camera's spectral responsivity and quantum efficiency will be measured using an intensity calibrated monochromator as light source.[9,10]
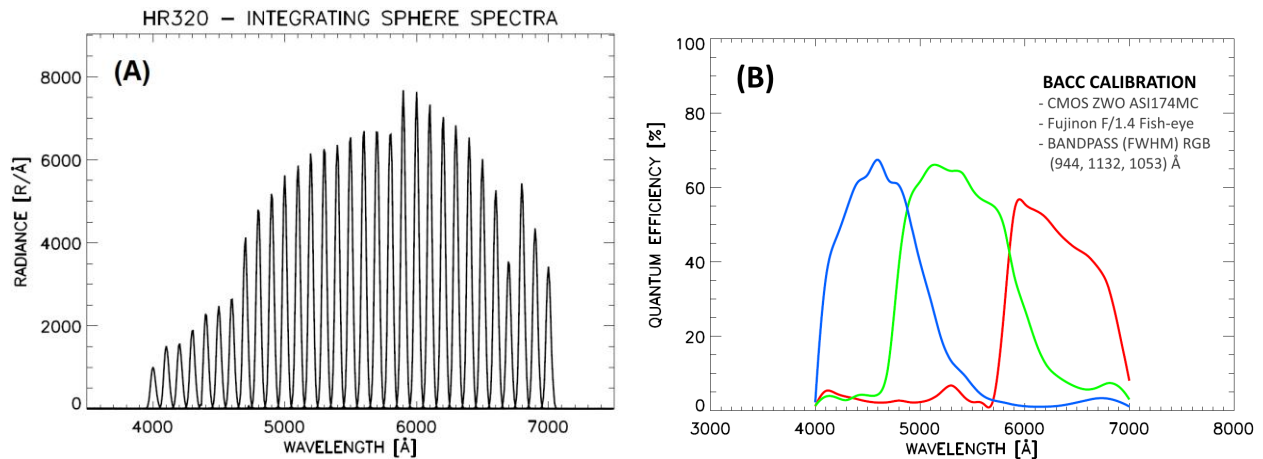
Fig. 4. Spectral calibration of the Boreal Aurora Camera Constellation (BACC). Panel (A) shows the 31 absolute calibrated integrating sphere source spectra used to obtain the quantum efficiency presented in panel (B). [9]

The experimental setup for spectral calibration consists of a fiber illuminator (Leica 150 W) that is connected to the entrance slit of a monochromator (Jobin Yvon HR320). The diffracted light at the exit slit of the monochromator is then fed into an integrating sphere. The output of the sphere is the target for both the BACC camera and an intensity calibrated FICS spectrograph (Fixed Compact Spectrograph from Oriel SN 7743).[9]

Figure 4 shows our first attempt to find the quantum efficiency of the camera. Our assembled wavelength tunable system is designed for the visible part of the spectrum (4000-7000 Å), producing monochromatic lines with a bandpass of ~12 Å. The calibrated FICS spectrograph measures the intensity of the integrating sphere output in units of R/Å. The bandpass of the spectrograph is Δλ≈50 Å. 31 absolute calibrated source spectra are shown in panel (A). The resulting Quantum Efficiency (QE) is shown in panel (B).

Note that, the QE is close in shape compared to the one provided by ZWO for the Sony Exmor IMX174 CMOS sensor, except for the blue channel. The level of the blue channel is ~10% too high. This is found to be connected to the default settings of the color balance of the camera. Consequently, the calibration will be repeated with unbalanced raw color channel output.

Calibration is vital for the project to make sure that the cameras in the proposed constellation are close to identical. It is also important to find the optimum color balance of the camera to develop an automatic routine to detect the aurora based on colors. See initial attempts section 6.
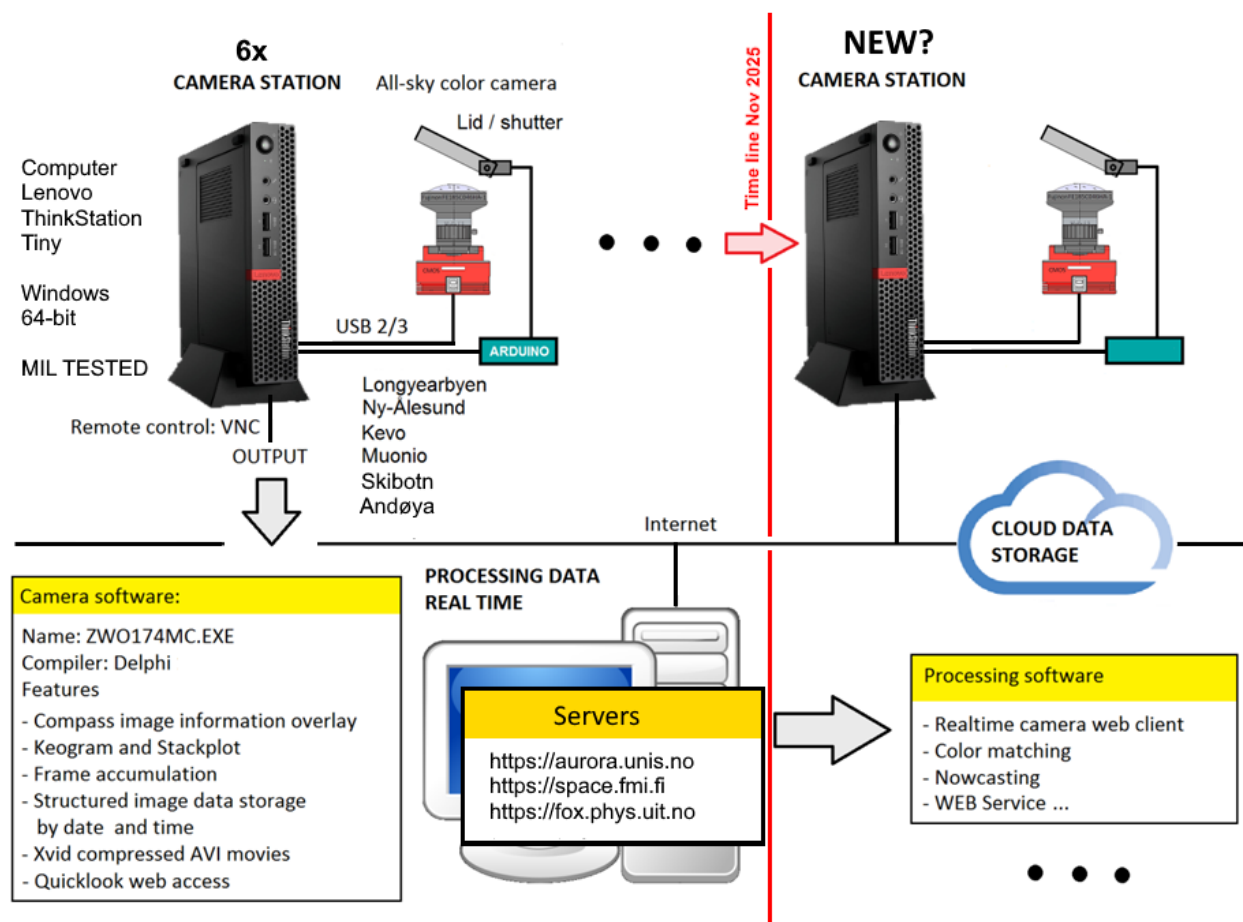
4. The camera network - constellation

Fig. 5. Sketch of the Boreal Auroral Camera Constellation (BACC).

Figure 5 summarized the architecture and the main idea behind the camera network. Much of the instrumental work in this proposal is already conducted. See left of the red time line in Figure 5. The main idea behind this proposal is to expand the network by deploying identical camera stations to multiple sites in the boreal zone.

First, Ny-Ålesund was an obvious candidate due to the distance and the high-speed internet fiber connection to Longyearbyen. An operational test period with dual site camera observations has been conducted from Longyearbyen and Ny-Ålesund in 2016. The test was important before an expansion to other similar sites is considered. The main site requirement is fast internet. The operators or institutions could be selected by interest and use of the network. The cost of operation and maintenance could also be part of the site institution's responsibility. The running costs are only the power consumption of one computer. The Department of Physics at the University of Oslo has now joined the constellation with a camera installed at the Sverdrup Research Station in Ny-Ålesund. The Finnish Meteorological Institute has also joined with two cameras at Muonio and Kevo in northern Finland operational in 2017. In 2020, Tromsø

Geophysical Observatory (TGO) joined with a camera at the Skibotn Observatory. The latest to join is Andøya Space with a camera at the Alomar Observatory. Camera #6 was operative in November 2025.
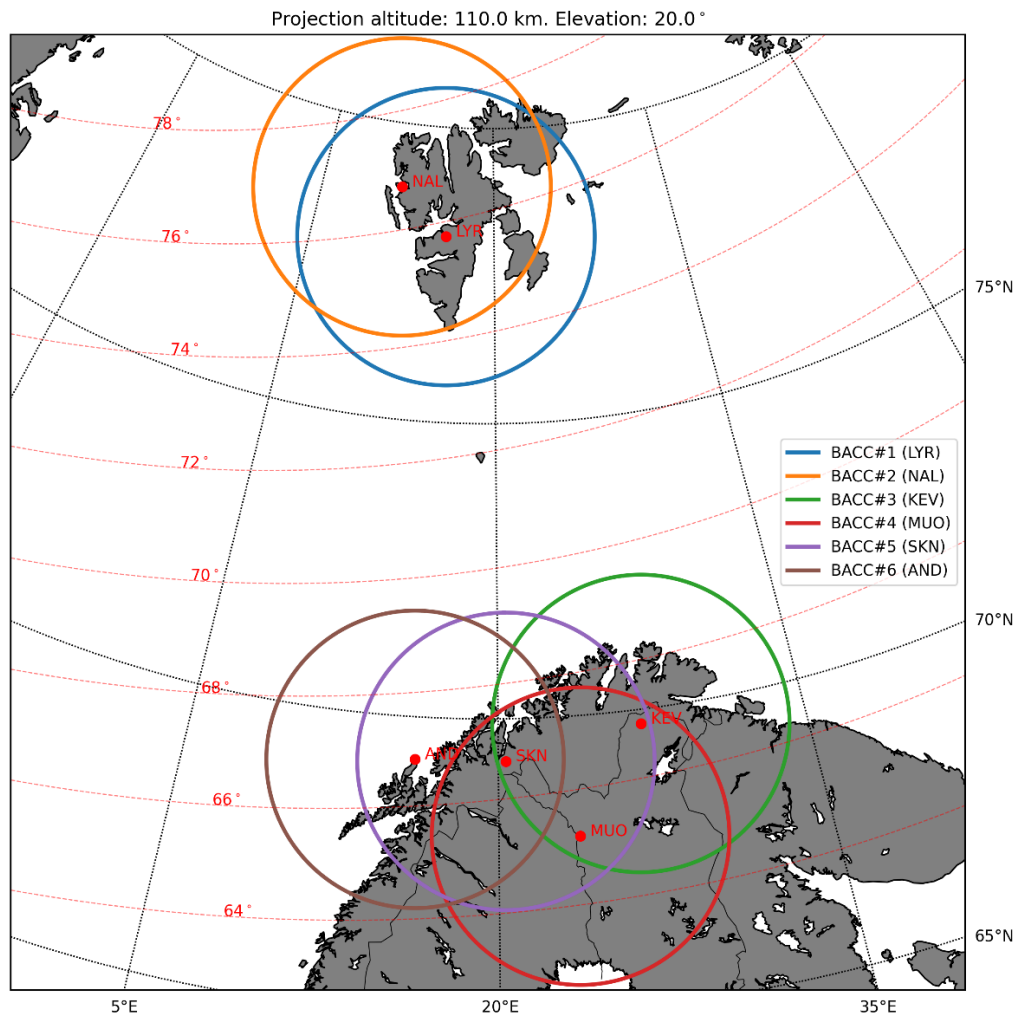
Fig. 6. Estimated Boreal Aurora Camera Constellation (BACC) field of view for 110 km peak emission altitude and blocking set to 20 degrees above the horizon. Camera station abbreviations: LYR – Longyearbyen, NAL – Ny-Ålesund, KEV – Kevo, MUO – Muonio, SKN – Skibotn and AND – Andøya.

Figure 6 shows the calculated all-sky field of view of the constellation assuming the aurora is located at peak emission altitude 110 km and 20 degrees above the horizon.

Real – time analysis of the network will include software development that is capable of color detection to be used as a now cast and verification of our forecast service. Feature and segmentation-based techniques may also prove to be helpful in the classification of auroral forms. Or in other words, what type of aurora that occurs. A large number of remote servers can access the data in real time and produce visual displays available to the general public. The data stream of the network will also serve the scientific community. Students may test their models in real time. Satellite, rocket and radar experiments will gain visual confirmation on auroral activity and weather conditions on a boreal scale.

UNIVERSITY CENTRE IN SVALBARD UNIS BOX 156 9171 LONGYEARBYEN NORWAY

5. Sample data
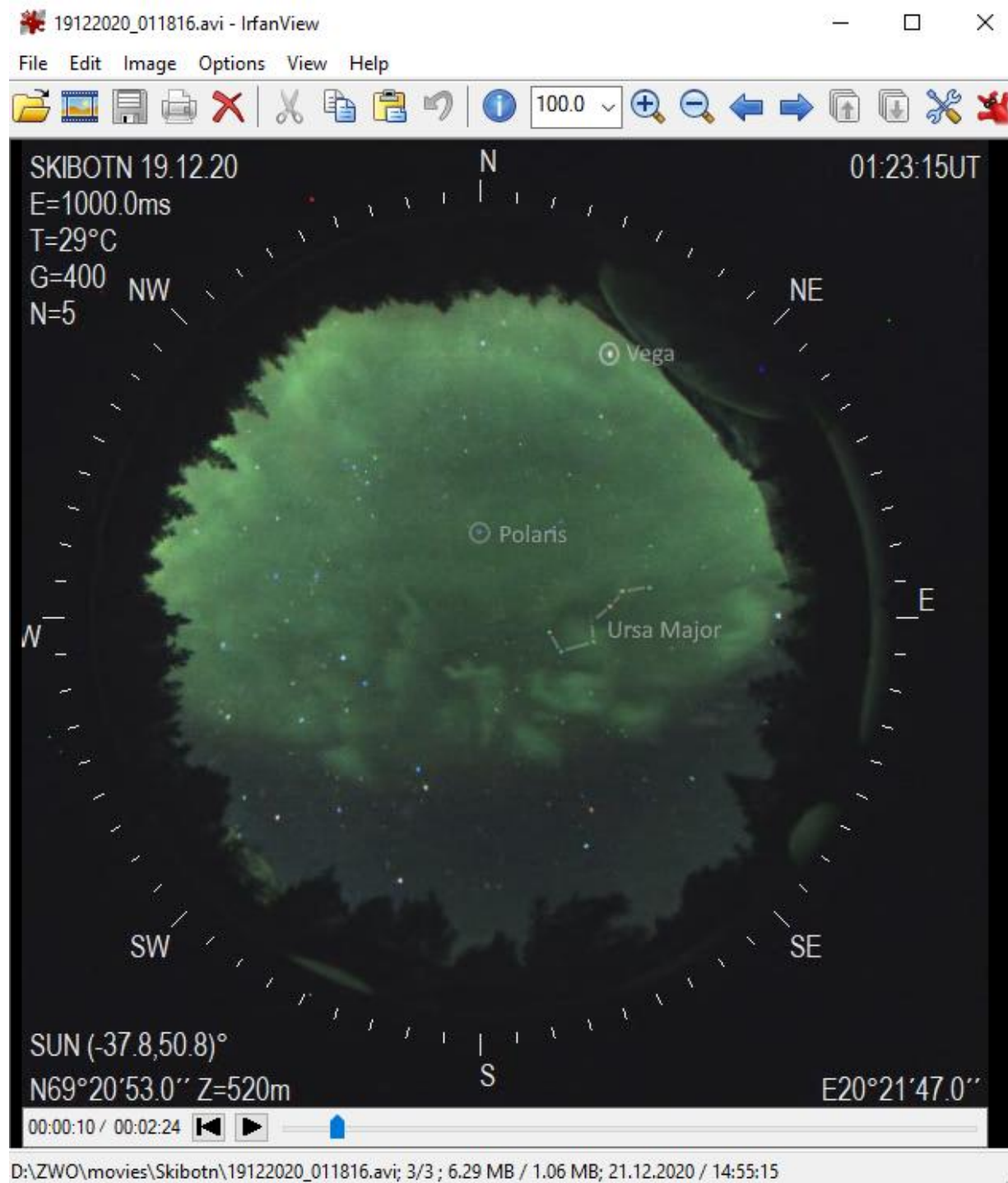
Fig. 7. All-sky color camera movie snapshot from the Skibotn Observatory (SKN) on 19th of December 2020. Typical post-midnight structured aurora related to night side sub storm.

First data sample is from the Skibotn Observatory on 19th of December 2020. A movie snapshot of a typical post-midnight structured aurora associated with a sub storm is shown in Figure 7.

UNIVERSITY CENTRE IN SVALBARD UNIS BOX 156 9171 LONGYEARBYEN NORWAY

Stars and constellations are easily identified by color and magnitude. In fact, the radial mapping function of the lens can be calculated directly from the snapshot. Also note that the light pollution at Skibotn is extremely low.

The Xvid compressed AVI movie contain 3600 frames. The exposure time is set to one second and the gain is set to automatic. 24 movies are made each day depending on the solar elevation. The size of the compressed movie is only ~6.5 Mbytes, which make it possible to store a whole auroral season of data on the camera PC without filling up the hard drive.
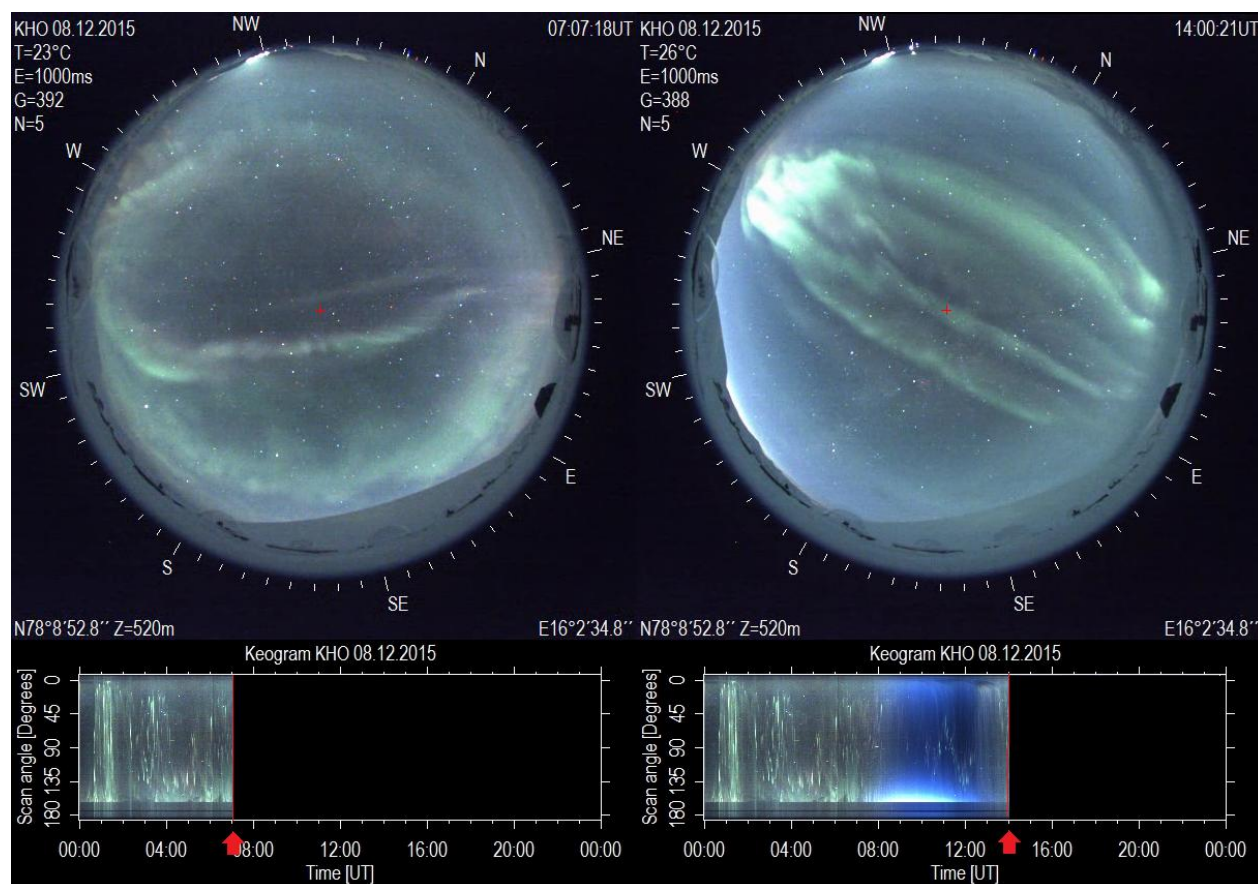
Fig. 8. All-sky color camera screen snapshots from the Kjell Henriksen Observatory (KHO) on 8th of December 2015. Left: Pre noon dayside aurora at 07:07:18 UT. A one hour movie of the pre noon event (Media 1). Right: Post noon auroral arcs at 14:00:21 UT. A one hour movie of the post noon event (Media 2). Keograms below marks time (red arrows) and activity across the magnetic meridian as a function of time for both snapshots.

Figure 8 shows snapshots of the camera from KHO on 8th of December 2015. Typical pre noon dayside auroral arcs are seen moving poleward with a more energetic green diffuse aurora to the south marking the open closed field line boundary. The diffuse or green aurora is believed caused by magnetically trapped high energy electrons leaking out of the loss cones by pitch angle scattering, causing particle precipitation into the upper atmosphere. This is classified as Type 3 aurora.[11] In the media file of Fig. 8, the diffuse dayside aurora shows clear sign of temporal and spatial dynamics, which contain information about plasma disturbances in the magnetosphere that has yet to be explored. This phenomenon is related to leakage of energized

UNIVERSITY CENTRE IN SVALBARD UNIS BOX 156 9171 LONGYEARBYEN NORWAY

electrons that in space weather terms is named the "killer electrons", due to the negative effect they have on space craft electronics.

The post noon situation shows multiple arcs classified as Type 5 aurora, related to the Region 1 current system that couples the polar ionosphere to the energy extraction from the solar wind.[11] The multiplicity of these arcs is interpreted as the auroral signature of kinetic Alfven waves propagating perpendicularly to the magnetic field.[12] Whether these arcs are on open or closed field lines are not clear, and it is a research subject of fundamental importance to space physics.

Identifying the overflying satellites and the use in-situ measurements could very well answer these questions. Satellites are easy seen in the camera as they are illuminated by the Sun. There is in other words, lots of detailed auroral information that can be studied with this camera.
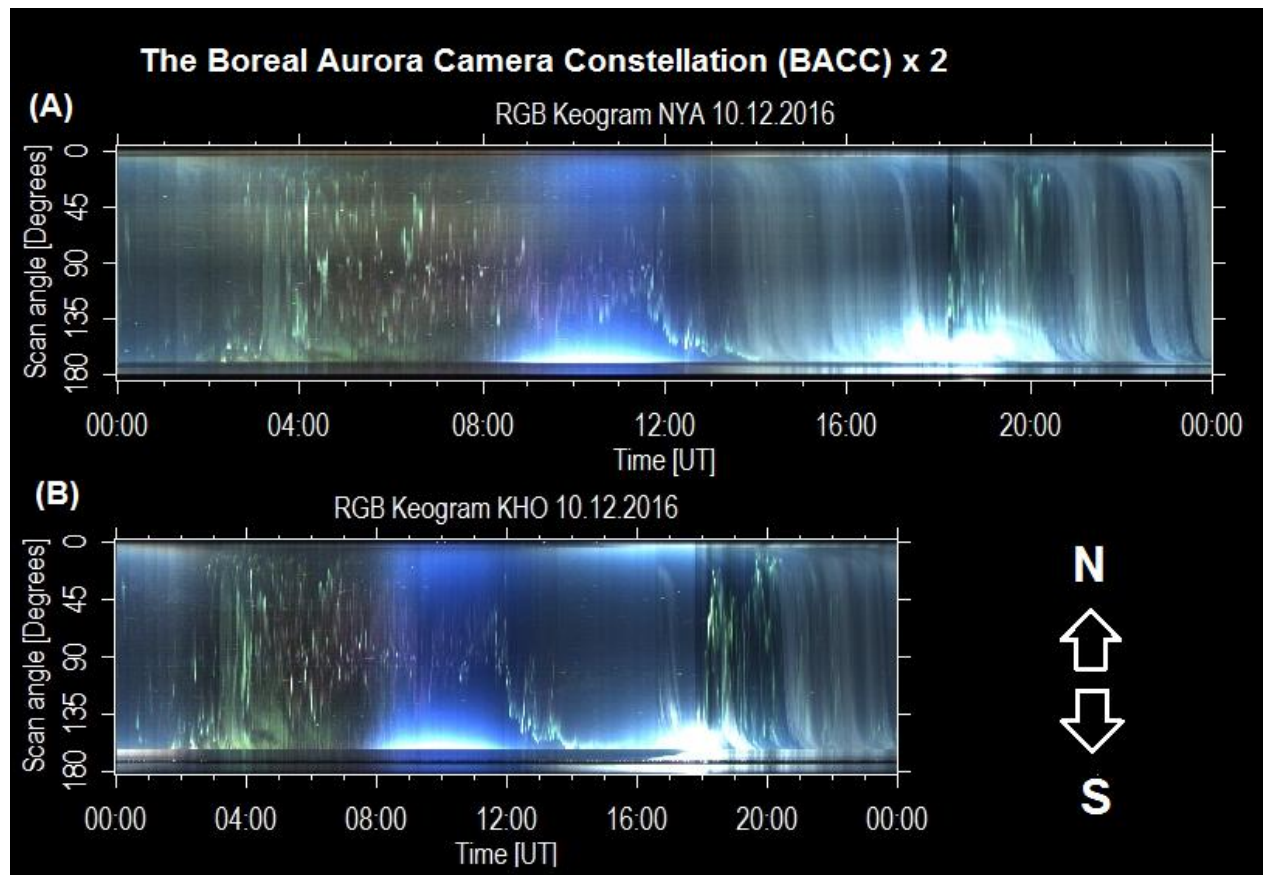
Fig. 9. BACC dual site keograms along the North – South magnetic meridian from Ny-Ålesund in panel (A) and from the Kjell Henriksen Observatory (KHO) panel (B), 10th of December 2016.

Figure 9 shows dual site keograms from 10th of December 2016. The second camera joining the constellation is operated by the Department of physics, University of Oslo, and is installed at the Sverdrup Research Station in Ny-Ålesund. Pre-noon, cusp and post-noon arcs are detected from

both sites with similar temporal signatures and colors. Also note that a cloud layer is seen moving from North to South, starting in Ny-Ålesund at ~14 UT moving over Longyearbyen 6 hours later.

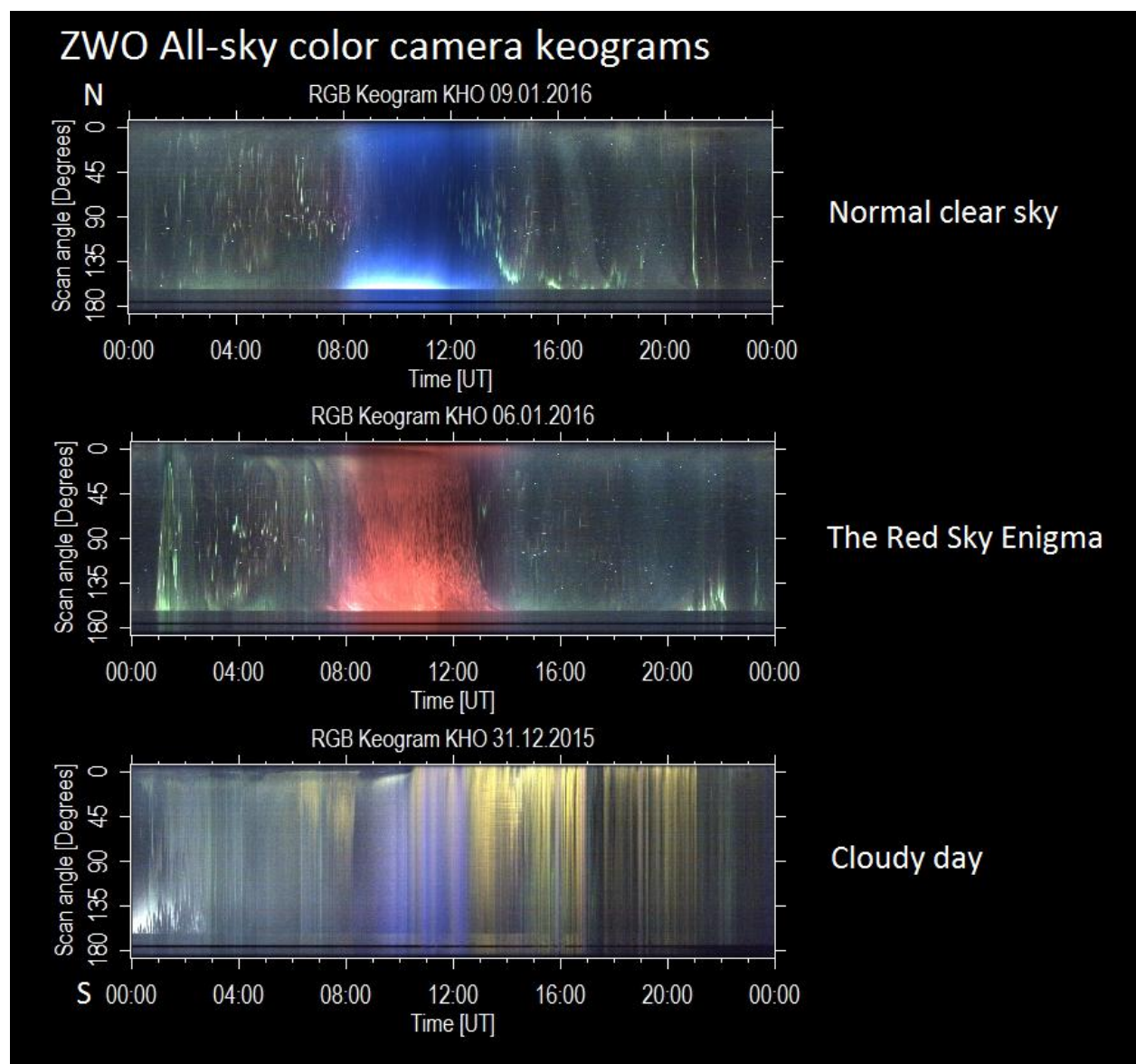**Fig. 10.** Daily all-sky color camera Keograms along the magnetic meridian from the Kjell Henriksen Observatory (KHO) illustrating normal clear sky (top), the Red Sky enigma (middle) and cloudy conditions (bottom) on 9th, 6th and 31st of December 2015, respectively.

The dual site data set is unique. It can be used to triangulate the altitude of the auroral arcs, which gives us an estimate the initial energy input of the precipitating source electrons. In addition, both the equatorward and the poleward boundaries of the auroral oval can be calculated. The latter enables us to update and improve our auroral forecast service, especially on the dayside where observations are sparse compared to nightside observations. The color balance of the camera could also be optimized to emphasize the red to green ratio of the

UNIVERSITY CENTRE IN SVALBARD UNIS BOX 156 9171 LONGYEARBYEN NORWAY

aurora, which ultimately could lead us to detect the open – closed field line boundary directly from the keograms.

In fact, the daily keograms of the camera reveal that the camera is capable of distinguishing between clear sky and cloudy conditions even in complete darkness. The effect is seen in Figure 10. Clouds tend to obscure, scatter, diffuse and even recolor any light sources being present. The aurora, the moon, Rayleigh scattered sun light mid-day and artificial light illuminate the clouds.

For these reasons, the camera could well be of interest to the meteorological community to quantify cloud coverage and type. Furthermore, high altitude clouds such has polar stratospheric ones are also clearly detected. They duct scattered solar light to Svalbard. This is known as the Red Sky Enigma that causes great public attention when they appear mid-winter.[13,14]

6. Color detection of aurora

Automatic detection of aurora based on color is a non-trivial task. Our hypothesis is that aurora has a unique color space that is separated from other light sources on the night sky. The wavelength of the overall brightest auroral emission line is at 557.7 nm. It originates from electron impact excitation of atomic oxygen [OI]. The lifetime of the emission is 0.7 second. The emission is clearly identified as green to the human eye.

Figure 12 shows an attempt to detect the aurora based on simple cake-sliced thresholding of the Hue Saturation Lightness (*HSL*) color space. The *HSL* color space is cylindrical in shape. The height of the cylinder defines intensity or *L* from black to white. A horizontal sliced circular disk of the cylinder is called a color wheel, where *H* represents the basic colors as a function of wheel angle in degrees. The radial distance from center of the wheel is *S* or purity (white mixed with *H*) of the color. *L* and *S* have decimal values in the range 0 to 1.

Fig. 11. Horizontal cross section of the HSL color space (color wheel): (H) Hue, (L) Lightness (L = 0.5), Saturation (S), and (C) color cake slice.

One of the main advantages by choosing the *HSL* color space is that the *H* component alone can be used to separate objects with different color, especially in situations when the illumination is non-uniform. The latter property is due to the fact that *H* is independent of intensity.[15]

In addition, gray-level algorithms can be applied directly to the *L* component. Table 1 demonstrates the non-uniform intensity effect of the *HSL* color space. The green target color *H* = 120° for different values of *S* and *L* are shown. It is hard to apply the same thresholds to the *RGB* space. *H*, *S* and *L* are all encoded into the *RGB* values. The computational complexity is simple and fast.

UNIVERSITY CENTRE IN SVALBARD UNIS BOX 156 9171 LONGYEARBYEN NORWAY

Fig. 12. HSL color matching of aurora: (A) The original 24-bit RGB image from the Kjell Henriksen Observatory (KHO) at 13:51:09 UT, 9th of January 2016, (B) color matched image, and (C) cake-slice section of HSL color wheel.
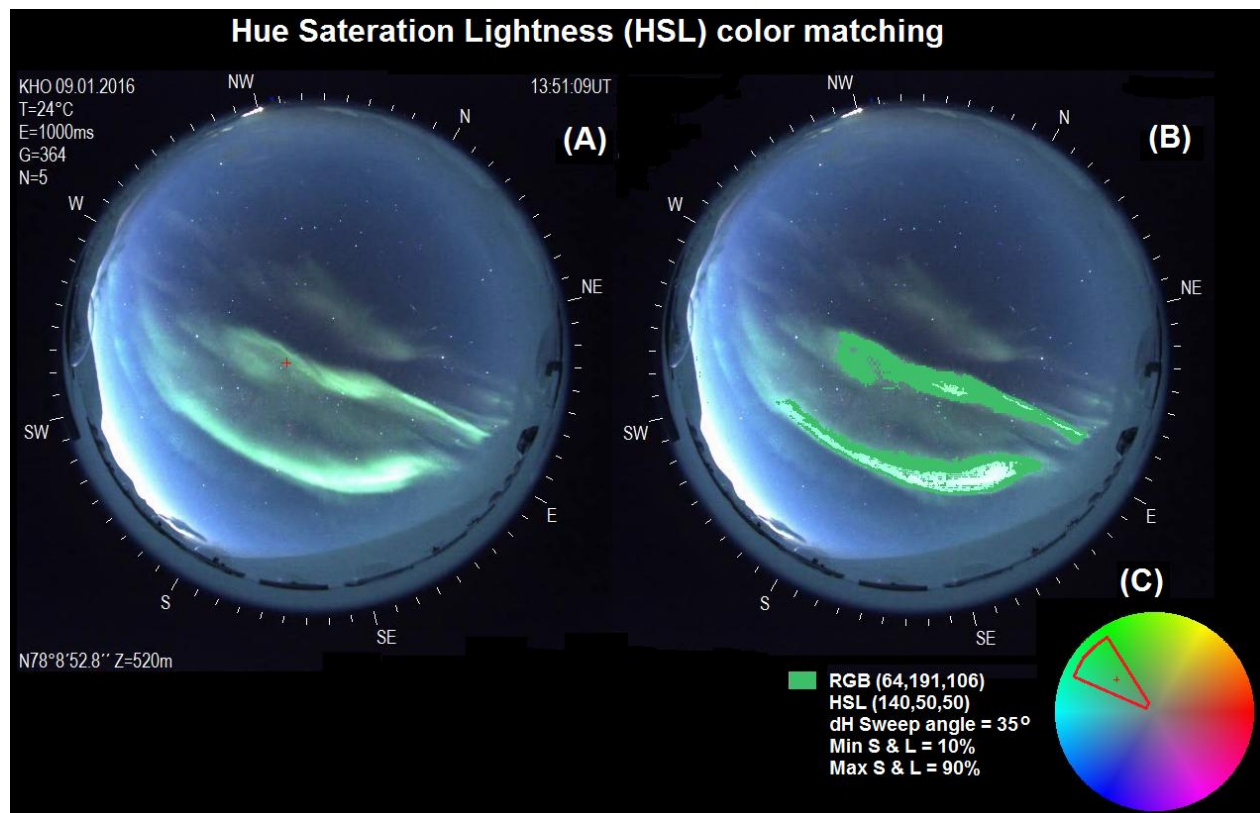
Color	R	G	B	H	S	L
	38	115	38	120	0.5	0.3
	64	191	64	120	0.5	0.5
	179	230	179	120	0.5	0.8

Table 1. *RGB* versus *HSL* color values

The disadvantages of the *HSL* color space is a non-removable singularity near the center axis of the color cylinder. A small change in input *RGB* values close to the center will cause large jumps in *HSL* transformed values. Also, if *L* is close to black or white in intensity, then color segmentation will fail regardless of *H* and *S*.

Another fast algorithm to detect color is to find the optimum palette for the aurora based on color clustering or reducing the colors of the 24-bit RGB images down to 8-bit. Due to hardware limitations on number of colors to display on a computer screen back in the 80's, the Graphics Interchange Format (GIF) developed by the company CompuServe Network, Inc. in 1987, provides optimized palette based methods to reduce high resolution color space images. The graphics format is now included in Delphi with GIF extensions and variable size palette optimization. Figure 13 shows how the GIF based color reduction works on the original 24-bit

frame in Figure 12, panel (A). 64 colors were manually recorded to form a custom-made palette representing non illuminated pixels (black), text (white), background sky conditions and aurora.
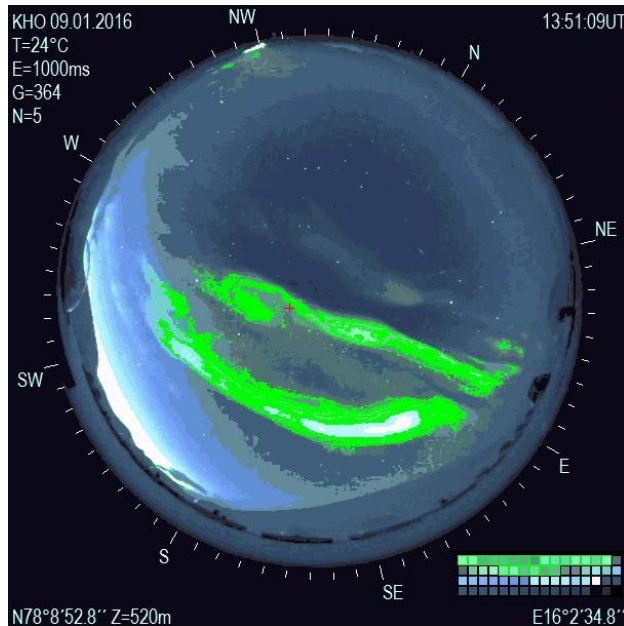
Fig. 13. Custom palette-based color matching of the aurora observed from The Henriksen Observatory (KHO) at 13:51:09 UT, 9th of January 2016. Lower right corner shows the 64-color palette used with 21 green marked colors classified as aurora.

The class of colors representing aurora is framed with the color light green in the palette. The detected auroral colors in the image are over painted with the same color.

The challenge of both methods is as mentioned above variable light conditions. For example, and increased background sky illumination (Rayleigh scattering) will affect the detected auroral colors. Or in other words, each frame in time has its own optimized palette. A multi selection of colors and palettes to form a library of possible scenarios will be tested to improve the detection of the target.

Furthermore, another solution might be to apply motion-based detection of the color clusters to extract the typical behavior or property of the target with time.

The aurora is in general large in size and moves quickly over the sky compared to the cloud cover, the rising sun, the moon and any light pollution sources.

7. High Dynamic Range (HDR) imaging

High dynamic range (HDR) images can be created in real-time by taking a series of bracketed images, i.e. images taken at different integration times. From a reference set of images, the camera response function is found using the method described by Debevec and Malik. [16] The camera response for the BACC cameras can be seen in Figure 14. As this response represents the conversion of a given radiance to counts of the chip, it is independent of the optical system in front on the chip.

The HDR image is simply the weighted sum of the radiance maps from each image in the exposure sequence.[16] Furthermore; the result is tone mapped to 24-bit prior to display. The example image shown in Figure 14 demonstrates the technique. 9 exposures were taken between 1 to 500 ms. The fastest exposures captured the outside light through the window without being overexposed, while the long exposures captured the inside dimmer office walls. The net result is an image that is not over- or under exposed. Note that the accumulation also decreases noise.
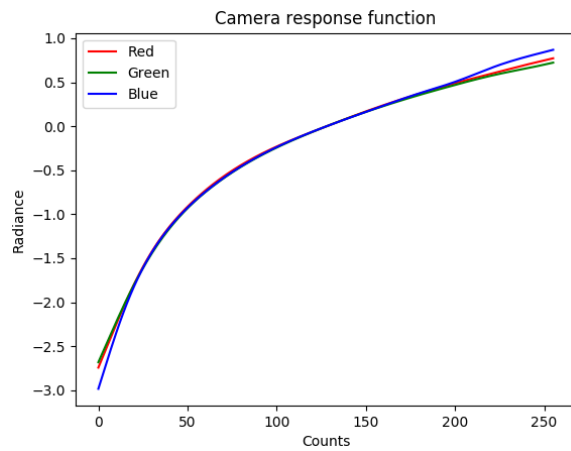
Figure 14. High Dynamic Range (HDR) imaging. Left panel: ASI174MC-Cooled camera response function.[16] Right panel: Office view HDR image constructed with 9 exposures at 1, 3, 7, 10, 50, 100, 200, 300 and 500 ms. The gain was set to 0. The aperture of the Fujinon lens was set to minimum F/16.

The net color balance in the HDR image is preserved, which in turn may improve the color detection algorithms in section 6.

8. Validation

Visual inspection of the processed frames will be matched by other instruments and techniques already present at KHO. Our hyperspectral all-sky cameras named NORUSCA can isolate the main auroral emission lines as function of wavelength. A successful classification of both dayside- and nightside auroras has been conducted.[17] The hyper- spectral data will be used to validate our color matching algorithms.

9. Parts and cost camera station

#	Item	Description	~Cost [kNOK]
1	Fujinon F/1.4 fish-eye lens	All-sky camera front optics	7
2	C-mount to T2 Extension ring	Lens to camera head adapter (Baader)	0.5
3	ZWO ASI174MC	Color CMOS camera head	5
4	C-Mount Brass Spacer Ring Kit	Used for fine focus and fixing of lens	0.7
6	Computer	PC Windows 64-bit	15
7	USB Cables	5m USB cable from computer	2
8	Software	VNC license / Delphi Rad Studio	6.5
9	Misc.	Packing, freight etc.	3.3
10	Calibration	Mounting, focus and sensitivity check	10
			Total 50

Table 2. Estimated cost of camera station's components and work.

UNIVERSITY CENTRE IN SVALBARD UNIS BOX 156 9171 LONGYEARBYEN NORWAY

10. Data storage

Essential for the project is to store all the data generated by the camera constellation and to provide visual displays for the public. Public data is defined as quick looks and keograms. The main raw data from each camera station is digital movies. The size of a one frame per second Xvid compresses AVI movie is approximately < 10 MBytes/hour. This is only ~7.5 GBytes per month. Transfers to secure data storage should be done daily. We propose that storage and access to the data is provided by all partners in the constellation. Furthermore, backups on a monthly scale should be of national interest to for example the Uninett Norstore facility.

11. Quick looks

#	Location	Latitude (deg.)	Longitude (deg.)	Partner	Latest data
1	Longyearbyen	78.150000	16.040000	KHO	Camera 1
2	Ny-Ålesund	78.923500	11.909900	UiO	Camera 2
3	Kevo	69.760000	27.010000	FMI	Camera 3
4	Muonio	67.958333	23.683333	FMI	Camera 4
5	Skibotn	69.348150	20.363310	UiT	Camera 5
6	Andøya	63.300000	16.010000	AS	Camera 6

Table 3. Location and latest data quick looks from BACC.

12. Third-party access

Data access to raw data or movies should be controlled by the Primary Investigator (PI) at each location. Any third party should reference and acknowledge the use of the data in a proper scientific manner and conduct as agreed with the PI. If the camera data is vital to any major scientific discovery, the site PI should insist on co-authorship on any published work. The latter is important to make sure that the data is presented correctly. PIs of several rocket campaigns have used data from the cameras. [18-21, 26-30]

One successful example of third-party co-operation is with Dr. Gerard Fasel at Pepperdine University in California, where students have full access to the BACC #1 archive from KHO. Detailed studies have been conducted on how Poleward Moving Auroral Moving Forms (PMAFs) connects to the dayside magnetosphere.[22, 31-34] Even a new type of twisted dayside aurora related to an extreme foreshock out in the magnetospheric bow has been discovered in the data.[23, 35, 36] It shows us how important it is to have a new set of eyes to study the rather huge and rapid expanding dataset from each camera.

13. Next steps?

The current constellation is located to cover Svalbard and northern Scandinavia. The Muonio, Kevo, Andøya and Skibotn cameras are perfectly located to cover any sky events for the new Eiscat 3D radar. An old dream to install cameras at Bjørnøya, Hopen or even Jan Mayen could be considered if we can find partners that have a genuine interest to join BACC. An expansion to the East would require a co-operation with the Polar Geophysical Institute (PGI) in Murmansk,

which is not likely to happen due to the war in Ukraine. But all alternatives need to provide a fast internet connection to join the constellation's real-time operational philosophy. Future expansion over to Iceland and Greenland could also be considered.

Summary

A low cost auroral all-sky color camera station has been constructed and tested. It is the core component of the proposed boreal auroral camera network - constellation. The network aims to provide multi-site real time all-sky data across the boreal zone to enable detailed studies of various sky phenomena. The constellation currently consists of cameras installed and operational in Longyearbyen, Ny-Ålesund, Skibotn, Andøya, Kevo and Muonio.

Where to apply funding: TBD

The constellation has expanded slowly with a low-cost philosophy and minimum administrative overload. More funding is needed if it is decided to expand faster. Funds for logistical costs including spare parts, is also needed to secure the constellation as it is. These are key questions we need to address before we decide how to move forward.

References

1. Sigernes, F., M. Dyrland, P. Brekke, S. Chernouss, D.A. Lorentzen, K. Oksavik, and C.S. Deehr, Two methods to forecast auroral displays, *Journal of Space Weather and Space Climate (SWSC)*, Vol. 1, No. 1, A03, DOI:10.1051/swsc/2011003, 2011.
2. Syrjäsuo M.T. and Donovan E.F., Diurnal auroral occurrence statistics obtained via machine vision, *Annales Geophysicae*, 22, 4, 1103-1113, 2004.
3. Partamies N., Syrjäsuo M. and Donovan E., Using colour in auroral imaging, *Canadian Journal of Physics*, 85, 2, 101-109, 2007.
4. Syrjäsuo M. and Partamies N., Numeric image features for detection of aurora, *IEEE Geoscience and Remote Sensing*, 9, 2, 176-179, 2012
5. Rao J., Partamies N., Amariutei O., Syrjäsuo M. and van de Sande K.E.A., Automatic auroral detection in color all-sky camera images, *IEEE Journal of Selected Topics in Applied Earth Observations and Remote Sensing*, 7, 12, 4717-4725, 2014.
6. Wacker, S., J. Gröbner, C. Zysset, L. Diener, P. Tzoumanikas, A. Kazantzidis, L. Vuilleumier, R. Stöckli, S. Nyeki, and N. Kämpfer (2015), Cloud observations in Switzerland using hemispherical sky cameras, *J. Geophys. Res. Atmos.*, *120*, doi: 10.1002/2014JD022643.
7. Brandstrom, B. U. E. C.-F. Enell, O. Widell, T. Hansson, D. Whiter, S. Makinen, D. Mikhaylova, K. Axelsson, F. Sigernes, N. Gulbrandsen, N. M. Schlatter, A. G. Gjendem, L. Cai, J. P. Reistad, M. Daae, T. D. Demissie, Y. L. Andalsvik11, O. Roberts, S. Poluyanov, and S. Chernouss, Results from the intercalibration of optical low-light calibration sources 2011, *Geosci. Instrum. Method. Data Syst.*, ISSN 2193-0856., 1(1), s 91-97, DOI: 10.5194/gid-1-91-2011, 2012.
8. Sigernes, F., S. E. Holmen, D. Biles, H. Bjørklund, X. Chen, M. Dyrland, D. A. Lorentzen, L. Baddeley, T. Trondsen, U. Brändström, E. Trondsen, B. Lybekk, J. Moen, S. Chernouss, and C. S. Deehr, Auroral all-sky camera calibration, *Geosci. Instrum. Method. Data Syst. Discuss.*, 4, 515-531, 2014.

9. Sigernes, F., Dyrland, M., Peters, N., Lorentzen, D., Svenøe, T., Heia, K., Chernouss, S., Deehr, C., and Kosch, M., The absolute sensitivity of digital colour cameras, *Opt. Express* 17, No. 22, 20211-20220, 2009.

10. Sigernes, F., J. M. Holmes, M. Dyrland, D. A. Lorentzen, T. Svenøe, K. Heia, T. Aso, S. Chernouss, and C. S. Deehr, Sensitivity calibration of digital colour cameras for auroral imaging, *Opt. Express* 16, 15623-15632, 2008.

11. Sandholt, P.E., C.J. Farrugia, J. Moen, Ø. Noraberg, B. Lybekk, T. Sten, and T.L. Hansen, A classification of dayside auroral forms and activities as a function of IMF orientation, *J. Geophys. Res.,*103, 23,325-23,345, 1998.

12. Moen, J., P. E. Sandholt, M. Lockwood, A. Egeland, and K. Fukui, Multiple, discrete arcs on sunward convecting field lines in the 14-15 MLT region, *J. Geophys. Res.*, 99, 6113-6123, 1994.

13. Sigernes, F., N. Lloyd, D.A. Lorentzen, R. Neuber, U.-P. Hoppe, D. Degenstein, N. Shumilov, J. Moen, Y. Gjessing, O. Havnes, A. Skartveit, E. Raustein, J. B. Ørbæk, and C.S. Deehr, The Red - Sky Enigma over Svalbard in December 2002, *Annales Geophysica,* 23, 1593-1602, 2005.

14. Lloyd, N. D., D. A. Degenstein, F. Sigernes, E. J. Llewellyn, and D. A. Lorentzen, A mechanism for the red-sky enigma: Ducting of sunlight by Polar Stratospheric Clouds, *Annales Geophysica,* 23, 1603-1610, 2005.

15. H. D. Cheng, X. H. Jiang, Y. Sun, and J. Wang, Color image segmentation: advances and prospects, *Pattern Recognition,* 34, 2259-2281, 2001.

16. Debevec, P. E. and J. Malik, Recovering high dynamic range radiance maps from photographs. SIGGRAPH 97 Conf. Proc., August 3–8, 1997.

17. Sigernes, F., Y. Ivanov, S. Chernouss, T. Trondsen, A. Roldugin, Y. Fedorenko, B. Kozelov, A. Kirillov, I. Kornilov, V. Safargaleev, S. Holmen, M. Dyrland, D. Lorentzen, and L. Baddeley, Hyperspectral all-sky imaging of auroras, *Opt. Express*, 20, 27650-27660, 2012.

18. Lessard, M.R, B. Fritz, B. Sadler, I. Cohen, D. Kenward, N Godbole, J. H. Clemmons, J H. Hecht, K. A. Lynch, M. Harrington, T. M. Roberts, D. Hysell, G. Crowely, F. Sigernes, M. Syrjäsuo, P. Ellingsen, N. Partamies, J. Moen, L. Clausen, K. Oksavik and T. Yeoman (2019), Overview of the Rocket Experiment for Neutral Upwelling Sounding Rocket 2 (RENU2), *Geophys. Res. Lett.*, 46, https://doi.org/10.1029/2018GL081885

19. N. H. Godbole, K. A. Lynch, M. Burleigh, M. R Lessard, L. B. N. Clausen, J. H. Clemmons, P. A. Fernandes, B. A. Fritz, M. Harrington, D. L. Hysell, D. R. Kenward, I. J. Moen, K. Oksavik, T. M. Roberts, F. Sigernes and M. D Zettergren, RENU2 Rocket Observations of Fine-Scale Thermal Ion Upflow, Downflow, and Temperature, *Earth and Space Science Open Archive*, 11, 2020, https://doi.org/10.1002/essoar.10503285.1

20. Chrystal Moser, James LaBelle, Spencer Mark Hatch, Jøran I. Moen, Andres Spicher, Toru Takahashi, Craig A Kletzing, Scott Randolph Bounds, Kjellmar Oksavik, Fred Sigernes and Tim Yeoman, The Cusp as a VLF Saucer Source: First Rocket Observations of Long-Duration VLF Saucers on the Dayside, *Earth and Space Science Open Archive*, 2020, https://doi.org/10.1002/essoar.10504347.1

21. C. Moser, J. LaBelle, S. Hatch, J. I. Moen, A. Spicher, T. Takahashi, C. A. Kletzing, K. Oksavik, F. Sigernes and T. K. Yeoman, The Cusp as a VLF Saucer Source: First Rocket

Observations of Long-Duration VLF Saucers on the Dayside, Accepted by GRL December 2020, https://doi.org/10.1029/2020GL090747

22. G.J. Fasel, J. Briggs, J. Mann, L.C. Lee, F. Sigernes, and Dag Lorentzen, More evidence that poleward-moving auroral forms are ionospheric signatures of magnetic reconnection, *Submitted to JGR-Space Physics*, Special Section: Results of the GEM Dayside Kinetics Southward IMF Challenge, 2019.

23. Jennifer Briggs, Gerard Fasel, Marcos Silveira, David Sibeck, Yu Lin, and Fred Sigernes, Solar-Terrestrial Interactions: Dayside Auroral Observation Resulting from a Rapid Localized Compression of the Earth's Magnetic Field, Vol 17 (19), *GRL*, 2020, https://doi.org/10.1029/2020GL088995

Conferences

24. Fred Sigernes, Dag A. Lorentzen, Magnar G. Johnsen, Torsten Aslaksen, Mikko Syrjäsuo, Stefan Wacker, Jakob Abermann, Bjørn Lybekk, Espen Trondsen, Lasse Clausen and Jøran Moen, The Boreal Aurora Camera Constellation (BACC), The 43nd Annual European Meeting on Atmospheric by Optical Methods, Winchester, UK, 15 -19 August, 2016.

25. Fred Sigernes, Mikko Syrjäsuo, Pål Gunnar Ellingsen, Bjørn Lybekk, Espen Trondsen, Lasse Clausen, Jøran Moen, Jyrki Mattanen and Kirsti Kauristie, Status: The Boreal Aurora Camera Constellation (BACC), The 44th Annual European Meeting on Atmospheric by Optical Methods, Barcelona, Spain, 4 - 8 September 2017.

26. D. A. Lorentzen, M. Conde, P.G. Ellingsen, L. Baddeley, F. Sigernes and D. L. Hampton, The C-REX sounding rocket experiment, MIST (Magnetosphere – Ionosphere – Solar Terrestrial Physics) meeting, Lancaster University, UK, April 2016.

27. Marc Lessard , Lasse Boy Novock Clausen, James H Clemmons, Ian Cohen, Pål Gunnar Ellingsen, Charles J Farrugia, Bruce Fritz, Meghan Harrington, Spencer Hatch, James H Hecht, David L Hysell, David Ross Kenward, James W Labelle, Kristina A Lynch, Jøran Idar Moen, Kjellmar Oksavik, Noora Partamies, Steven P Powell, Brent Sadler, Fred Sigernes, Mikko Syrjäsuo, and Timothy K Yeoman, Observations of Poleward Moving Auroral Forms by the Rocket Experiment for Neutral Upwelling 2 (RENU2) Sounding Rocket (Invited), AGU Fall meeting 2016, San Francisco, USA.

28. James H Clemmons , James H Hecht, Douglas G Brinkman, Marc Lessard, David L Hysell, Kristina A Lynch, Meghan I Harrington, Kjellmar Oksavik, Jøran Idar Moen, Fred Sigernes, Timothy K Yeoman, and Bruce Fritz, Structure of the Thermosphere during Energy Input through the Magnetospheric cusp: Measurements from the RENU2 Ionization Gauge, AGU Fall meeting 2016, San Francisco, USA.

29. David Ross Kenward , Marc Lessard, Kristina A Lynch, David L Hysell, James H Hecht, James H. Clemmons, Geoff Crowley, Ian J Cohen, Fred Sigernes, Kjellmar Oksavik, Timothy K Yeoman, Sun-Hee Lee, and James L Burch, Cusp Electron Populations During a Neutral Upwelling Event: Measurements from RENU2 and MMS Conjunction, AGU Fall meeting 2016, San Francisco, USA.

30. Marc Lessard, T. A. Bekkeng, Lasse Boy Novoc, Clausen, James H Clemmons, Geoff Crowley, Pål Gunnar Ellingsen, Bruce Fritz, Meghan I Harrington, Spencer Hatch, James H Hecht, David L Hysell, David Ross Kenward, James W Labelle, Kristina A Lynch, Jøran Moen, Kjellmar Oksavik, Antonius Otto, Noora Partamies, Steven P Powell, Brent Sadler, Fred Sigernes, Mikko Syrjäsuo and Timothy K Yeoman, The "Rocket Experiment for Neutral Upwelling 2 (RENU2)" Sounding Rocket, AGU Fall meeting 2016, San Francisco, USA.

31. Gerard Fasel, Kate Kononenko, Ashley Rothballer, Alexandra Angelo, Mashaer Alyami, Taylor Brandt, Benjamin Fox, Alexander Grissom, Michael Gribble, Kristine Lysenstoen, Fred Sigernes, Dag Lorentzen, David Green, and Maxwell Freeman: A Study of the Different classes of Poleward-Moving Auroral Forms, AGU Fall meeting, 14 – 18 December, San Francisco, USA, 2015.

32. G.J. Fasel, J. Briggs, J. Mann, F. Sigernes, and D. Lorentzen, Poleward-moving auroral forms and their connection to the solar wind speed, AGU Fall meeting, 9 – 13 December, San Francisco, USA, 2019.

33. G.J. Fasel, L.C. Lee, J. Mann, J. Briggs, K. Butler, F. Sigernes, and D. Lorentzen, East-West Brightening in Poleward-Moving Auroral Forms and the Interplanetary Magnetic Field By –Component, AGU Fall meeting, 9 – 13 December, San Francisco, USA, 2019.

34. K. Butler, G.J. Fasel, J. Briggs, A. Mascot, L. Hickmann, M. Kim, J. Mann A. Merritt, A. Nguyen, A.D. Oneto, S. Zhou, Fred Sigernes, and Dag Lorentzen, Dayside Auroral Oval Shifts Due to Enhanced Solar Wind Dynamic Pressure, AGU Fall meeting, 9 – 13 December, San Francisco, USA, 2019.

35. Jennifer Briggs, David Sibeck, Marcos Silveira, Gerard Fasel, Sun Hee Lee, Mike Ruohoniemi, John Mann, Fred Sigernes, and Dag Lorentzen, Ionospheric Response to a Transient Event at the Magnetopause, AGU Fall meeting, 9 – 13 December, San Francisco, USA, 2019.

36. Media Event

Aurora Seashell!   December 24, 2019

Jennifer Briggs, a physics student at Pepperdine University in Malibu, has analyzed our BACC data and discovered a new type of twisted dayside aurora related to an extreme foreshock out in the magnetosphere.

Links: **NASA statement**, **Space.com** and **Forbes**

APPENDIX

(A) BACC CAMERA V1 [LYR – NAL – KEV – MUO – SKN – AND]

#	Item	Model	Part link	Description
1	Sensor head	Sony Exmor IMX174	ZWO ASI174MC	1936x1216 pixels (5.86 μm)
2	All-sky lens	Fujinon F/1.4 Fisheye	FE185C057HA-1	FOV 185º (ø5.7 mm)
3	Lens adapter	Baader Extension ring	#2958521	M42x0.75 male T-thread to female C-mount threads

(B) BACC CAMERA V2 [HELSINKI]

#	Item	Model	Part link	Description
1	Sensor head	Sony STARVIS Exmor R	ZWO ASI178MC	3096x2080 pixels (2.4 μm)
2	All-sky lens	Fujinon F/1.4 Fisheye	FE185C046HA-1	FOV 185º (ø4.6 mm)
3	Lens adapter	Watec spacer ring	WAT-34CMA-R	5 mm Spacer Ring
4	Brass spacers	Edmund Optics	Spacer Rings	0.25-0.X mm thick

(C) SUN SHIELD V1-V2

#	Item	Model	Part link	Comment
1	Lid	3D printed	LensCover.STL	Lens cover lid
2	Servo clamp	3D Printed	ServoClamp.STL	Servo attachment to lens
3	Servo	Parallax Standard	#900-00005	0-180º range (4-6V)
4	Controller	Arduino	UNO	Serial COM controlled (USB)